Orbital element generation for an optical and laser tracking object catalogue

J. C. Bennett
Space Environment Research Centre, Mt Stromlo Observatory, Cotter Road, Weston Creek ACT 2611 AUSTRALIA
C. Smith
EOS Space Systems Pty Ltd, Mt Stromlo Observatory, Cotter Road, Weston Creek ACT 2611 AUSTRALIA
B. Greene, D. Kucharski
Space Environment Research Centre, Mt Stromlo Observatory, Cotter Road, Weston Creek ACT 2611 AUSTRALIA
F. Rigaut, F. Bennet,
Research School of Astronomy & Astrophysics, Australian National University, Mt Stromlo Observatory Cotter Road, Weston Creek ACT 2611 AUSTRALIA
J. Sang
School of Geodesy and Geomatics, Wuhan University, 129 Luoyu Road, Wuhan, 430079, CHINA

ABSTRACT

In this paper results are presented from an analysis assessing the data requirements for orbit element generation for a new high-accuracy catalogue for the Space Environment Research Centre, Australia. The analysis is working towards obtaining a robust set of rules for orbit element generation using orbital data from optical and laser tracking of debris and satellites.

Optical and laser tracking data collected from several tracking campaigns carried out by EOS Space Systems Pty Ltd, located on Mount Stromlo, Australia, is fitted to provide an updated orbital element. The element accuracy is determined for various data-availability scenarios, including: (1) fitting optical tracking data only; (2) fitting optical and laser tracking data. The orbit predictions from the new orbital element are compared with SGP4 propagation from two-line element data and accuracy is assessed by comparing with high accuracy ephemerides where available or subsequent accurate tracking data. Future integration and enhancements to the catalogue are also discussed.

This work forms part of the collaborative effort of the Space Environment Management Cooperative Research Centre which is developing new technologies and strategies to preserve the space environment (www.serc.org.au).

1. INTRODUCTION

In this paper, we consider recent developments for a future space object catalogue for near-Earth orbiting objects from a planned network (under construction) of optical and laser tracking stations in Australia.

A new tracking site is being installed in Western Australia through a collaboration between Electro Optic Systems (EOS) and Lockheed Martin[1] with the support of the Australian Department of Defence. This is the first stage of construction for an Australian optical and laser debris tracking network. The goal of the network is to complement existing radar-based tracking systems such as the US Air Force's Space Fence. Along with the existing site on Mt Stromlo, ACT (which is fully operational), the first stage construction is the beginning of the network expansion.

The focus of this paper is the orbital element and propagation accuracy that is achievable from sparse optical and laser ranging tracking data. Results are presented for a single-station which shows that an improvement is gained in orbit prediction accuracy. Also considered is a brief simulation comparing the accuracy of an orbital element and propagation created from single-station tracking or tracking data from two stations.

[1] http://www.lockheedmartin.com.au/au/news/press-releases/2014/25082014.html, accessed 10 September 2015.

In the examples that follow, simple orbital elements are considered, derived from fitting (sparse) optical and laser tracking data from Mt Stromlo, and consist of an orbital state (epoch, radius, and velocity vector) with an estimation of the object's area-to-mass ratio. For objects in lower regions of the low-Earth orbit where atmospheric drag is the dominant non-gravitational perturbing force, the area-to-mass ratio is determined from drag effects using the method described in [1]. In higher orbits, the area-to-mass is derived from a new method developed within SERC that considers the effects of solar radiation effects on an orbit.

2. THE COOPERATIVE RESEARCH CENTRE FOR SPACE ENVIRONMENT MANAGEMENT

The Cooperative Research Centre for Space Environment management (SEMCRC), managed by the Space Environment Research Centre, was formed through the Australian Government's Cooperative Research Centre (CRC) program[2]. The Centre was officially launched[3] by Minister Ian Macfarlane on December 2nd, 2014 at Parliament House in Canberra, Australia, and is designed to build on Australian and international expertise and experience to develop cutting-edge technologies for the preservation of the space environment. SERC is an international partnership between EOS Space Systems Pty Ltd (AUS), RMIT University (AUS), ANU University (AUS), Lockheed Martin (US), Optus (AUS), and NICT (JPN). More details may be found at www.serc.org.au.

3. NETWORK

Currently, the only operational site in the planned network is the optical and laser tracking station at EOS Space Systems Pty. Ltd., located on top of Mount Stromlo, Canberra. The optical tracking system has a pointing precision of 1.5-2 arc-seconds root-mean squared (RMS) error from a mount model solution, and ~0.5 arc-seconds (RMS) using an astrometrics (star-catalogue) solution. The debris laser ranging system has range accuracy to approximately 1-1.5 metres and can track uncooperative objects (without retro reflectors). The optical and laser tracking systems are fully integrated and operate together. This results in the collection of accurate 3-dimensional observations when both systems are used to track an object.

Stage 1 of the network construction will see a new station located in Western Australia. The new station will also be an optical and laser debris tracking station and deliver accurate 3-dimensional tracking data of orbital debris objects. A map of the two stations is indicated in Fig. 1.

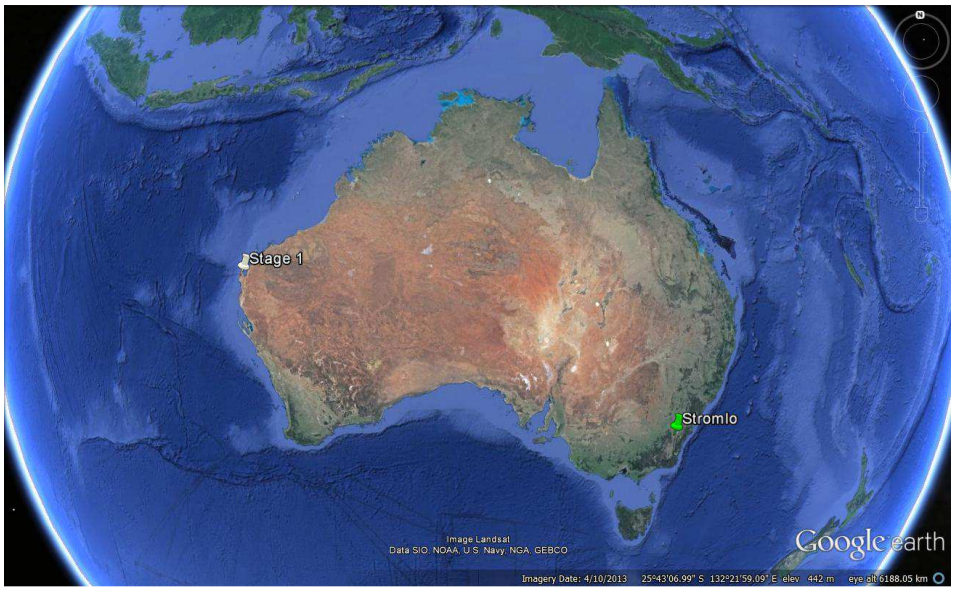

Fig. 1. Map indicating the location and distance between Stromlo and stage 1 of the ADTN construction. The baseline distance between the 2 sites is approximately 3,500 km

[2] http://crca.asn.au/, accessed 10 September 2015.
[3] http://www.minister.industry.gov.au/ministers/macfarlane/media-releases/australia-host-global-space-research-group-keep-satellites, accessed 10 September 2015.

4. COVERAGE

To evaluate the coverage that site 1 and 2 have for the current TLE catalogue, a visibility analysis was run to determine the proportion of objects that the sites have access to (i.e. they are trackable) during the morning and evening terminator periods for each object. The TLE catalogue was obtained for day 245 2015 from www.space-track.org and a visibility analysis performed for all objects with a TLE in the dataset. In total there were 10,044 TLEs used in the analysis.

Considering an elevation mask of 20 degrees, the Stromlo site had access to track 56% of these objects during a 4 week period. Similarly, the WA site had access to 50% of the objects for the day 245 catalogue. Combined, these sites had access to 59% of these objects. If the system could track outside of terminator conditions then these statistics would increase significantly.

5. ORBIT DETERMINATION

Significant progress has been made producing reliable orbit predictions (OPs) from sparse optical and laser tracking data in LEO [2, 3] and it has been shown that sufficient accuracy for unaided debris laser ranging is achievable [4]. The advances are due to a method to estimate the ballistic coefficient of the debris using long-term TLE data [1].

More recently, analyses investigating the minimum data requirements for reliable LEO OP from sparse, very short-arc tracklets have found that as little as two 5 seconds passes separated by 24 hours is sufficient when fitting optical and laser observations [5]. The accuracy and minimum data requirements are dependent on the availability of the range observations from the laser system and the angles (azimuth and elevation) observations from the optical system. If either of these is not available for an OD fitting then the results are not as reliable, indicating the importance of 3-dimensional observational data. Data fusion with TLE pseudo-observations has also been investigated and the weakly-weighted TLEs provide sufficient constraining for an otherwise indeterminate system caused by the lack of observational data [5]. A similar detailed analysis is due to be performed for HEO debris objects; however in this case we will only have the angular observations available.

In the next Section, we consider results from a method that has been developed recently as part of the CRC to help characterize debris objects outside regions where atmospheric drag is the dominant non-gravitational perturbing force, i.e. where the method described in [1] is not suitable.

6. ESTIMATING THE AREA-TO-MASS RATIO FROM SOLAR RADIATION PRESSURE EFFECTS

In this Section, preliminary test results are presented from a method developed recently to estimate an object's area-to-mass ratio using the effects of solar radiation on its orbit. The method uses long-term TLE data to estimate the perturbation induced on an object in an orbit where solar radiation is the dominant non-gravitational perturbation.

Tab. 1 shows the results of the method for 3 geodetic satellites: Ajisai, Etalon-1 and Etalon-2. The parameter γ is the radiation coefficient defined as $\gamma = C_R \frac{A_\odot}{m}$, where $A_\odot$ is the cross-sectional area in the sun-satellite direction, C_R is the reflectivity, and m is the mass of the object.

Tab. 1. Results comparing the area-to-mass ratio estimation method for spherical geodetic satellites.

		Truth data					Estimated	
NORAD ID	**Name**	**Shape**	D [m]	A [m^2]	m [kg]	A/m [m^2/kg]	Est. γ [m^2/kg]	Est. C_R
16908	Ajisai	Sphere	2.15	3.63	685	5.3e-3	6.3e-3	1.18
19751	Etalon-1	Sphere	1.294	1.32	1415	9.3e-4	8.9e-4	0.96
20026	Etalon-2	Sphere	1.294	1.32	1415	9.3e-4	8.9e-4	0.95

The results from the area-to-mass ratio method are shown in the "Estimated" columns. The estimated γ is resultant from the method and the estimated C_R is found by dividing it by the known area-to-mass. The method appears to be working well as the resulting values for C_R are realistic and the consistency between Etalon-1 and Etalon-2 is very encouraging. It appears this method is producing reasonable results and in the next section the method is tested in an orbit determination process to see if the value that results from the method yields good results. The performance of the method for non-spherical objects is being examined and the method will be adapted to handle these objects, in particular, high area-to-mass objects.

7. SIMPLE ORBIT ELEMENT TESTS

In this section, we consider simple orbital elements generated from the optical and laser tracking data from Mount Stromlo. In the low-LEO (defined here as the 200 – 900 km altitude region) examples presented, the CRC orbital element is defined as the position, velocity, and ballistic coefficient derived from the method in [1]. In higher LEO regions (above 900 km), the ballistic coefficient is replaced with the radiation coefficient determined from the effects of solar radiation. Note, in these orbit propagations no distinction is made between the cross-sectional area in the ballistic coefficient and radiation coefficients, i.e. they are assumed equal. This assumption will become more important in an orbit near the transition between solar radiation dominance to atmospheric drag dominance, and for objects with irregular aspect-ratios. In future revisions, this assumption will be relaxed. In the HEO cases, the ballistic coefficient is replaced with the radiation coefficient.

The objects are assumed to be spherical and only information gathered from the long term TLE data is used to characterize the object's area-to-mass ratio in the orbit determination. No other object-specific information is used.

The following section presents results for 4 separate objects:

1) TIROS-10: A low-LEO debris object with perigee altitude 717 km;
2) OPS-4311: A low-LEO debris object with perigee altitude 765 km;
3) NOAA-4: A LEO debris object with negligible drag effects with perigee altitude 1,444 km;
4) Object-A: A GEO object with perigee 35,714 km.

In all of these cases the CRC orbital element was generated from tracking data from Mt Stromlo only. A summary of the element creation regime are listed in Tab. 2.

Tab. 2: Summary information for the examples considered to show the CRC orbital element accuracy generated from sparse data.

Case #	Name	OD span (days)	OD start epoch (UTC)	# optical passes	# laser passes	A/m source	Tracking mode
1	TIROS-10	4	24/04/2013 00:00:00	4	4	Ballistic coefficient	Mount model
2	OPS-4311	4	24/04/2013 00:00:00	4	4	Ballistic coefficient	Mount model
3	NOAA-4	2	14/05/2012 00:00:00	2	0	Solar Radiation Coefficient	Mount model
4a	Object A	2	30/04/2015 00:00:00	2	0	Solar Radiation Coefficient	Mount model
4b	Object A	9	30/04/2015 00:00:00	4	0	Solar Radiation Coefficient	Mount model

In the following Section the accuracy of the propagation from the CRC orbital element is reported for the cases displayed in Tab. 2 against results from SGP4 propagation from the last available TLE in each case.

Note: In what follows, the results comparing the propagation of the TLE with SGP4 with the CRC orbital element propagation are not a fair comparison. The SGP4 propagator is an analytic propagator and therefore is much faster than the numerical integrator that is used with the CRC orbital element. Also the CRC element uses extra tracking data to correct the TLE. The comparison is made regardless since typically for debris objects the TLE and the SGP4 propagator is the method used to obtain an orbit prediction and the following results show the accuracy that can be gained by fitting sparse optical and laser tracking data.

7.1 Single station fitting

Fig. 2 shows a comparison between an orbit propagation from a CRC orbital element and SGP4 propagation from a TLE element for TIROS-10. The orbit prediction from each is compared to subsequent accurate angles and range (where available) tracking data collected from Mt Stromlo. The first plot shows the combined pointing residuals, indicating how close the object would have been to the boresight of the telescope for reacquisition. The second plot shows the range difference compared to the subsequent range observations.

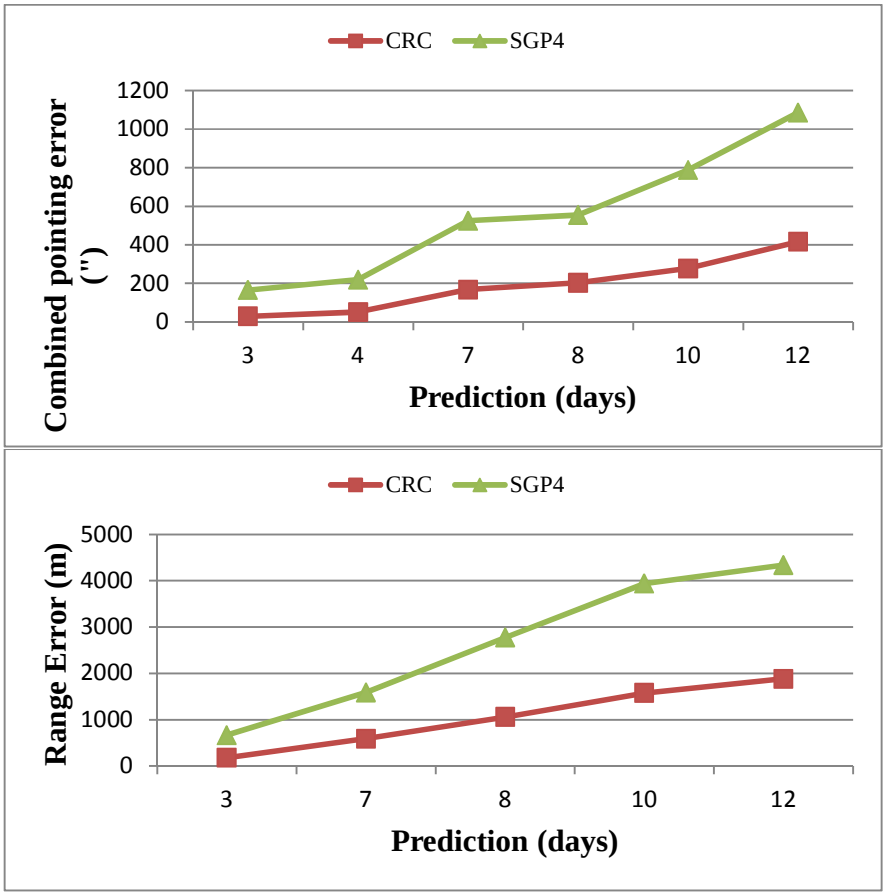

Fig. 2: Prediction results comparing propagation using a CRC orbital element with one using a TLE orbital element and the SGP4 propagator

Fig. 2 shows that the CRC orbit propagation performs better than the SGP4 propagation. The first plot shows the angular displacement from the subsequent observations. For a camera system with a narrow field of view (FoV) of 5.1 arc-minutes, the CRC element would be still visible after 10 days prediction. Comparatively, if we were to use the TLE+SGP4 propagation to cue the telescope, the object would not fall in the narrow FoV after approximately 5 days.

Tab. 3: Catalogue information for object TIROS-10 with NORAD ID 1430

Intl. Des.	NORAD ID	Name	Period	Inclination	Apogee	Perigee	RCS
1965-051A	1430	TIROS 10	100.0	98.1	800	717	0.8047

Fig. 3 shows the same comparison as Fig. 2 except for OPS-4311, details listed in Tab. 4. The CRC orbit element propagation leads to an improved prediction with the pointing error after 2 days being 19 arc-seconds compared with the SGP4 prediction of 63 arc-seconds. The CRC element would be sufficient for unaided laser ranging, subject to an experiment with a diverged laser beam for acquisition. If this were successful this would lead to accurate debris laser ranging out of terminator conditions.

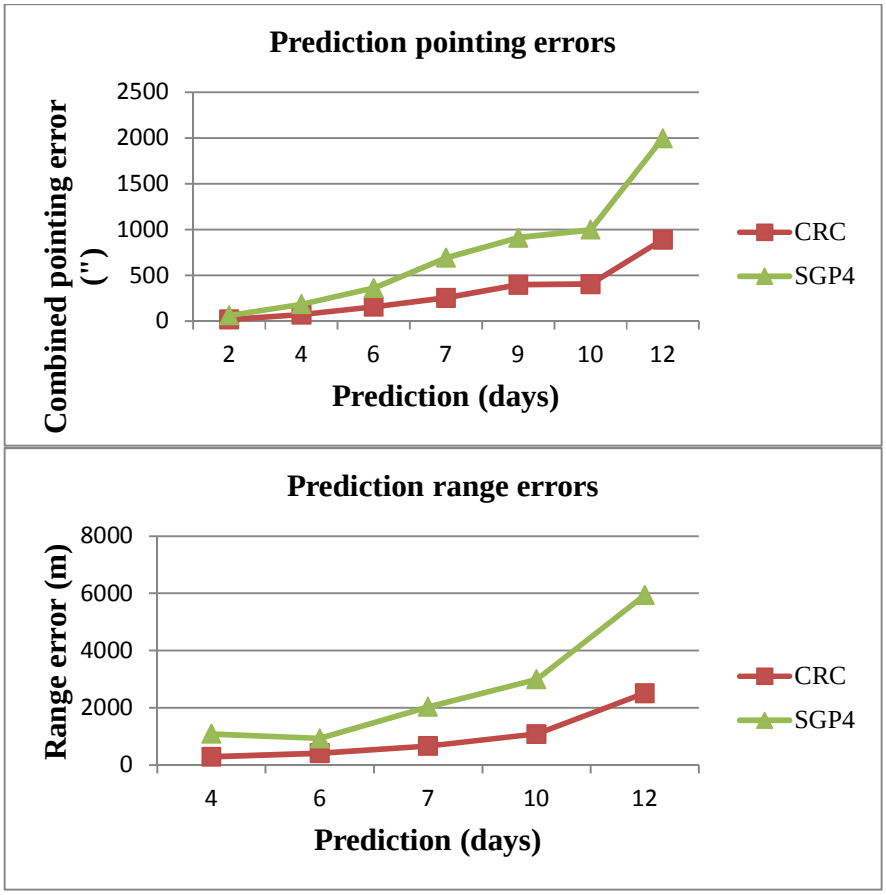

Fig. 3. Residuals comparing the orbit prediction from SGP4 propagation and CRC propagation. The top figure shows the combined pointing error and the bottom plot shows the range error. Note, there were no range observations collected for comparison for 2.4 and 9.4 day predictions.

Tab. 4 Catalogue information for object with NORAD ID 5557

Intl. Des.	NORAD ID	Name	Period	Inclination	Apogee	Perigee	RCS
1971-087A	5557	OPS 4311 (DMSP 5B F1)	100.9	99.1	840	765	1.2515

To test the validity of the area-to-mass ratio estimation from solar radiation effects, an orbit determination test was performed. An updated orbital element was generated by fitting 2 passes of angular track data from the Mt Stromlo site using a TLE as an initial state. During the orbit determination, two estimates of the area-to-mass ratio where trialed and held fixed, i.e. not estimated from the data fitting. These values were: (1) the estimate derived from the area-to-mass estimation method from the effects of solar radiation pressure; (2) the averaged value derived from the B^* data from all of the historical TLE data (note most of these values are set to 1e-4 in the TLE data set, which may be a default value).

Fig. 4 shows the results that test the validity of the area-to-mass ratio method. This shows the orbit prediction results for the object, with details listed in Tab. 5, for three cases: (1) "OD SF AM" shows the results of a numerical propagation from an orbital element generated from fitting 2 observational passes using the area-to-mass ratio derived from solar radiation effects; (2) "OD B*" shows the same as (1) except it uses the area-to-mass ratio derived from the TLE data; and, (3) SGP4 propagation from the last available TLE.

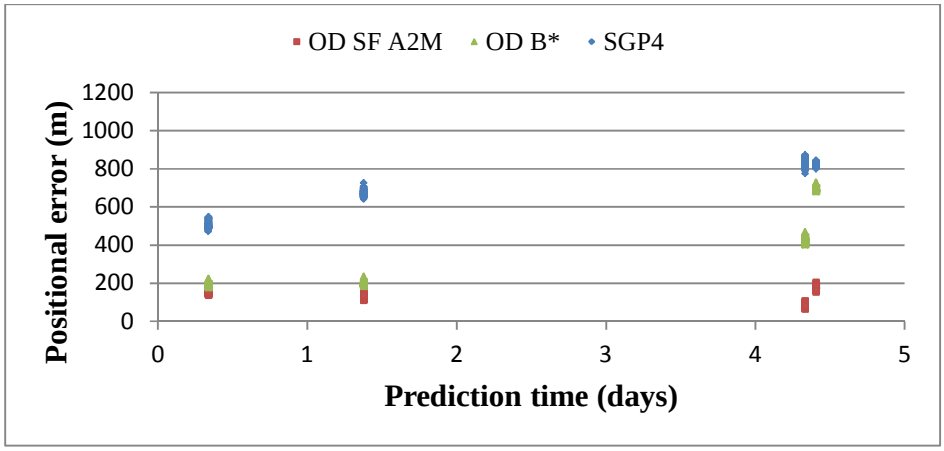

Fig. 4: Example of the accuracy improvement using an area-to-mass ratio derived from solar radiation effects for the object in Tab. 5. "OD SF A2M" signifies the area-to-mass ratio was used (fixed) in the orbit fit, "OD B*" signifies the average B* value from the TLE data was used to derive the area-to-mass, and "SGP4" is SGP4 propagation from the last TLE in the fitting period.

Tab. 5: Catalogue information for object with NORAD ID 7529

Intl. Des.	NORAD ID	Name	Period	Inclination [deg]	Apogee [km]	Perigee [km]	RCS
1974-089A	7529	NOAA 4	114.9	101.5	1459	1444	2.8143

Next, we consider the results for an object in GEO. Fig. 5 shows the results that test the validity of the area-to-mass ratio method. This shows the orbit prediction results for the object for three cases: (1) "2d" shows the results of a numerical propagation from an orbital element generated from fitting 2 observational passes using the area-to-mass ratio derived from solar radiation effects (and not estimating it during the OD process); (2) "9d" shows the same as (1) except the OD is performed over a 9-day period; and, (3) shows the same as (2) but estimating C_R from the observation data.

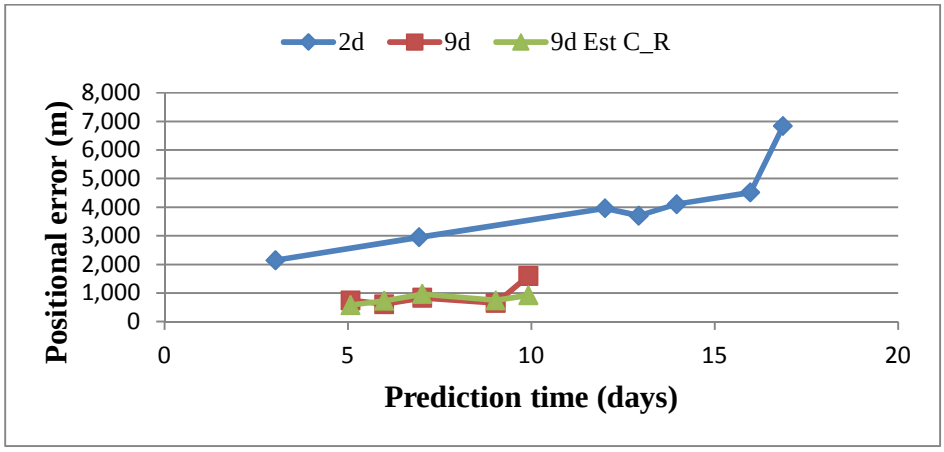

Fig. 5: Results from the GEO OD study. "2d" is the result of a 2-day OD fit (1 optical observation pass per day) and holding C_R constant; "9d" is a 9-day OD fit (with a total of 4 optical passes) and holding C_R fixed; and "9-d Est C_R is the same as "9d" except C_R is estimated during the OD.

These results show that our results are also reasonable for non-spherical objects. Overall, fitting C_R in the OD process yielded the best results; however, in data sparse scenarios, fitting C_R may lead to poor orbit predictions. A detailed study must be performed to identify when a data sparse scenario exists.

In what follows, we briefly look at the accuracy improvement that adding an extra tracking station can provide by performing a simulation study for a HEO object.

7.2 Two station simulations

Here we consider the improvements gained in introducing a second station to complement the Mt Stromlo site. In this analysis the second station was (arbitrarily) assumed to be located at Yarragadee, WA.

An orbit determination and prediction study was performed using simulated data. A reference orbit was used to generate simulated azimuth, elevation and range observations. For illustration of a HEO object, an accurate International Laser Ranging Service Consolidated Prediction Format (CPF) orbit solution for Etalon 1 was chosen as the reference. Simulated observations were then generated every 2 seconds for all periods where the object was sun-illuminated and visible from the tracking station. The observations were then corrupted with pseudorandom zero-mean Gaussian errors. Each azimuth and elevation observation was corrupted with random errors X_{az}, X_{el}, respectively, where $X_{az} \sim N(0, (0.5")^2)$, $X_{el} \sim N(0, (0.5")^2)$, where $N(\mu, \sigma^2)$ is the Normal (Gaussian) distribution, μ is the mean and σ is the standard deviation. The result is a set of 2-dimensional simulated observations for all visible periods where the object is sunlit. Subsets of this total data set were then selected to perform the simulation OD analysis.

The standard data abundance assumed was one 60 second pass per day is collected from each station. So the total data set is reduced so that this condition was met.

A batch least-squares OD procedure was used to determine the orbits fitting either single-station data or data from both over a 7-day fit span. The starting epoch of the OD simulation study was selected arbitrarily as 1st March 2015 and 20 simulations were performed sequentially, with the OD start epoch increasing by 1 day for each simulation. For all of the simulations a TLE was used as the initial state in the OD and a 30-day orbit prediction was determined from the converged OD solution. No object information was used other than that provided from the HEO area-to-mass ratio estimation method.

The observations were fitted using 11th order Cowell integration with a 30 second time-step, fitting a full orbital perturbing force model considering solar radiation pressure effects, Earth gravitational effects which are modelled using a 100×100 EIGEN-GL05C gravity model [6]. The ocean tidal effects are included through the CSR 3.0 ocean

tidal model [7], and the solid Earth tidal force is computed using the specification given in [8]. Third body gravitational forces are computed using the DE200 planetary ephemeris.

For each simulation run, the OD solution was propagated for 30 days after the end of the OD window with the area-to-mass ratio held fixed. Whether to estimate C_R during the OD process is important and therefore has received detailed attention for sparse data cases; however, this analysis is deferred to a later publication where it will be presented in detail with a study considering real tracking data.

The prediction was compared with the accurate CPF data to determine the Euclidean distance (position difference) every 1 minute. The maximum position difference each day for the orbit prediction was computed for all of the simulations and then averaged to obtain the results presented below. This is effectively the averaged "worse-case scenario" since the maximum error in each simulation was selected as the accuracy assessment metric.

Fig. 6 shows a comparison between the orbit prediction results from fitting data from 1 station (Mt Stromlo) with fitting data from 2 stations to assess the accuracy improvement from adding a second station.

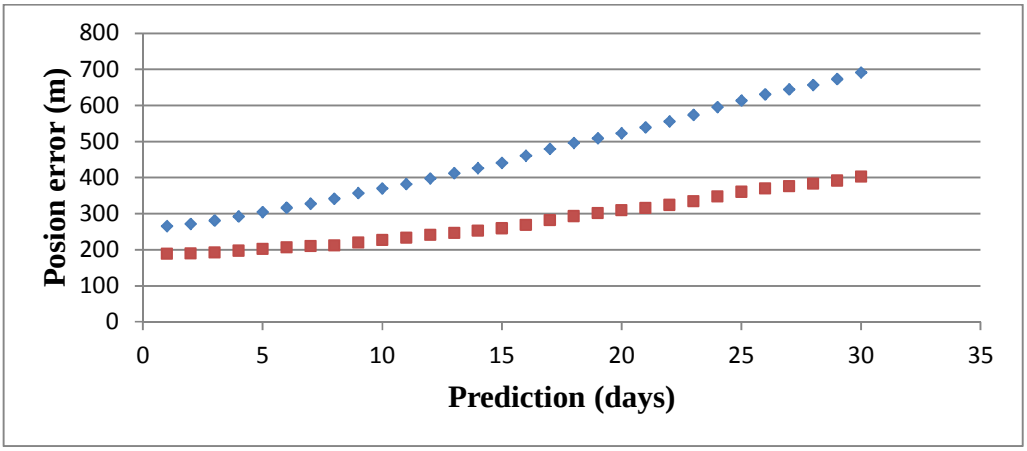

Fig. 6: Comparison showing this 3-dimensional Euclidean distance between the reference CPF orbit and (1) an orbit determined from fitting one 60 second pass per day from Stromlo only (blue stars); and, (2) an orbit determined from fitting one 60 second pass per day each from Stromlo & Yarragadee (red squares). In both, a 7 day OD was performed and C_R was *not* estimated.

From this figure it is clear that a second station improves the prediction results. As the network develops a campaign to assess the accuracy over multiple orbital regimes will be performed.

8. SYSTEM INTEGRATION AND FUTURE ENHANCEMENTS

The results considered in this paper are not representative of the anticipated accuracy of the catalogue since research developments are yet to be integrated. The accuracy will improve as these are integrated.
In moving from a case-by-case orbit analysis for individual orbiting objects to an integrated tracking and catalogue system care must be taken not to corrupt the orbit elements with tracking data containing errors. Quality control of observed data will be applied before elements are updated.

Spin orientation and rate, derived from light curves, will be used to enhance the accuracy of the catalogue and predictions. The spin parameters of defunct satellites equipped with retro-reflectors will be measured by both photometry and satellite laser ranging. The spin analysis from laser ranging will be used to parameterize and verify the photometric methodology for use on the wider population of objects.

The CRC space object catalogue will progressively include improvements in object characterization; such as the improved photometry through adaptive optics (see AMOS 2015 paper by F.Bennet et al. and [9]), spin rate and orientation, and area-to-mass ratio estimation. This is expected to lead to improved orbit predictions.

As more tracking stations are added to the network, multi-sensor tasking optimization methods can be deployed to maximize the accuracy of the catalogue. The current methods used to task the Mt Stromlo station will be adapted so that an optimal solution is achieved..

ACKNOWLEDGMENT

The authors of this paper wish to acknowledge funding for this research project from the Cooperative Research Centre for Space Environment Management (SERC Limited).

REFERENCES.

1. Sang, J., J.C. Bennett, and C.H. Smith, *Estimation of ballistic coefficients of low altitude debris objects from historical two line elements.* Adv. Space Res., 2013. **52**(1): p. 117-124.
2. Sang, J., J.C. Bennett, and C. Smith, *Experimental results of debris orbit predictions using sparse tracking data from Mt. Stromlo.* Acta Astronautica, 2014. **102**(0): p. 258-268.
3. Sang, J. and J.C. Bennett, *Achievable debris orbit prediction accuracy using laser ranging data from a single station.* Advances in Space Research, 2014. **54**(1): p. 119-124.
4. Bennett, J.C., et al., *Accurate orbit predictions for debris orbit manoeuvre using ground-based lasers.* Adv. Space Res., 2013. **52**(11): p. 1876-1887.
5. Bennett, J.C., et al., *An analysis of very short-arc orbit determination for low-Earth objects using sparse optical and laser tracking data.* Advances in Space Research, 2015. **55**(2): p. 617-629.
6. Förste, C., et al., *EIGEN-GL05C - A new global combined high-resolution GRACE-based gravity field model of the GFZ-GRGS cooperation.* Geophys. Res. Abstr., 2008. **10, EGU2008-A-03426**.
7. Eanes, R.J. and S. Bettadpur, *The CSR 3.0 global ocean tide model: diurnal and semi-diurnal ocean tides from TOPEX/Poseidon altimetry*, in *Technical Memorandum*. 1995, Center for Space Research.
8. McCarthy, D.D. and G. Petit, *IERS Conventions (2003)*, in *IERS Technical Note 32*. 2004, Frankfurt am Main: Verlag des Bundesamts für Kartographieund Geodäsie.
9. Bennet, F., et al. *Adaptive optics for space debris tracking*. 2014.